A Response Regulatory Protein with the Site of Phosphorylation Blocked by an Arginine Interaction: Crystal Structure of Spo0F from *Bacillus subtilis*[†,‡]

Madhusudan, James Zapf, James A. Hoch, and John M. Whiteley

Department of Molecular and Experimental Medicine, The Scripps Research Institute, 10550 North Torrey Pines Road, La Jolla, California 92037

Nguyen H. Xuong and Kottayil I. Varughese*

Department of Biology, University of California at San Diego, La Jolla, California 92093-0359

Received May 29, 1997; Revised Manuscript Received August 7, 1997[⊗]

ABSTRACT: Spo0F is a secondary messenger in the "two-component" system controlling the sporulation of *Bacillus subtilis*. Spo0F, like the chemotaxis protein CheY, is a single-domain protein homologous to the N-terminal activator domain of the response regulators. We recently reported the crystal structure of a phosphatase-resistant mutant Y13S of Spo0F with Ca^{2+} bound in the active site. The crystal structure of wild-type Spo0F in the absence of a metal ion is presented here. A comparison of the two structures reveals that the cation induces significant changes in the active site. In the present wild-type structure, the carboxylate of Asp11 points away from the center of the active site, whereas when coordinated to the Ca^{2+}, as in the earlier structure, it points toward the active site. In addition, Asp54, the site of phosphorylation, is blocked by a salt bridge interaction of an Arg side chain from a neighboring molecule. From fluorescence quenching studies with Spo0F Y13W, we found that only the amino acid Arg binds to Spo0F in a saturable manner (K_d = 15 mM). This observation suggests that a small molecule with a shape complementary to the active site and having a guanidinium group might inhibit phosphotransfer between response regulators and their cognate histidine kinases.

Bacteria, plants, and some lower eukaryotic organisms recognize and respond to environmental changes through the action of two-component signal transduction systems (Stock et al., 1990; Swanson et al., 1994; Alex et al., 1996). Two-component systems typically consist of a sensor histidine protein kinase and a response regulator; the sensor kinase recognizes the signal and responds by mediating the phosphorylation of the response regulator at the receiver domain (Parkinson & Kofoid, 1992). In response to poor growth conditions such as nutrient deprivation or high cell density, some bacteria will halt normal cell division and begin the developmental process of sporulation, leading to heat-resistant, refractile spores. Sporulation in *Bacillus subtilis* is controlled by a phosphorelay, an expanded version of the two-component system (Burbulys et al., 1991; Hoch, 1993). In this case, one or more protein kinases (KinA or KinB) autophosphorylate an internal histidine residue and this phosphoryl moiety is transferred to Asp54 on the response regulator Spo0F (Zapf et al., 1996; Stock et al., 1990), a single-domain protein with 124 amino acids. The phosphoryl moiety is ultimately transferred to another response regulator, Spo0A, from Spo0F-P through the activity of the phosphotransferase Spo0B. Phosphorylation of the N-terminal receiver domain of Spo0A allows the C-terminal DNA binding (output) domain (Grimsley et al., 1994) to function both as a repressor of growth-promoting genes and as an activator of genes required for sporulation. The phosphorelay is unusual among two-component signal transduction systems in that phosphotransfer occurs between two response regulators, Spo0F and Spo0A, through the action of the unique phosphotransferase Spo0B. The flow of phosphate from KinA or KinB to Spo0A is controlled by a sophisticated regulatory mechanism which involves the action of specific phosphatases (Perego et al., 1994; Perego & Hoch, 1996) .

The response regulator family of proteins has nearly 100 known members (Volz, 1993, 1995), and a mutant Spo0F, a nitrate response regulator NarL, and a chemotaxis response regulator CheY have had crystal structures defined at high resolution (Madhusudan et al., 1996b; Stock et al., 1989, 1993; Volz & Matsumura, 1991; Bellsolell et al., 1996; Baikalov et al., 1996). NMR studies on CheY (Moy et al., 1994; Santoro et al., 1995) have confirmed that the solution structure of this protein is very similar to the crystal structures. The global fold of the receiver domain of nitrogen response regulator NtrC has also been determined by NMR, giving a low-resolution structure (Volkman et al., 1995). The general protein fold of the receiver domain is similar for all these response regulator structures, consisting of a five-strand parallel β-sheet core in the arrangement $\beta2-\beta1-\beta3-\beta4-\beta5$ that is sandwiched by helixes $\alpha1$ and $\alpha5$ on one side and $\alpha2-\alpha4$ on the other side. The active site of Spo0F is formed at the carboxy end of the β-strands by residues Asp10, Asp11, Asp54, Thr82, and Lys104 (Figure 1A,B). The equivalent residues in CheY are Asp12, Asp13, Asp57, Thr87, and Lys109. In the Ca^{2+}-bound mutant structure, the cation is coordinated to the carboxylate of Asp11, Asp54,

[†] This investigation was supported in part by Grants GM54246, GM19416, and GM54727 from the National Institutes of Health.

[‡] The atomic coordinates of the model have been deposited with the Brookhaven Protein Data Bank under accession number 1NAT.

* To whom correspondence should be sent: Department of Molecular and Experimental Medicine, NX-1, The Scripps Research Institute, 10550 N. Torrey Pines Rd., La Jolla, CA 92037.

[⊗] Abstract published in *Advance ACS Abstracts,* October 1, 1997.

S0006-2960(97)01276-2 CCC: $14.00

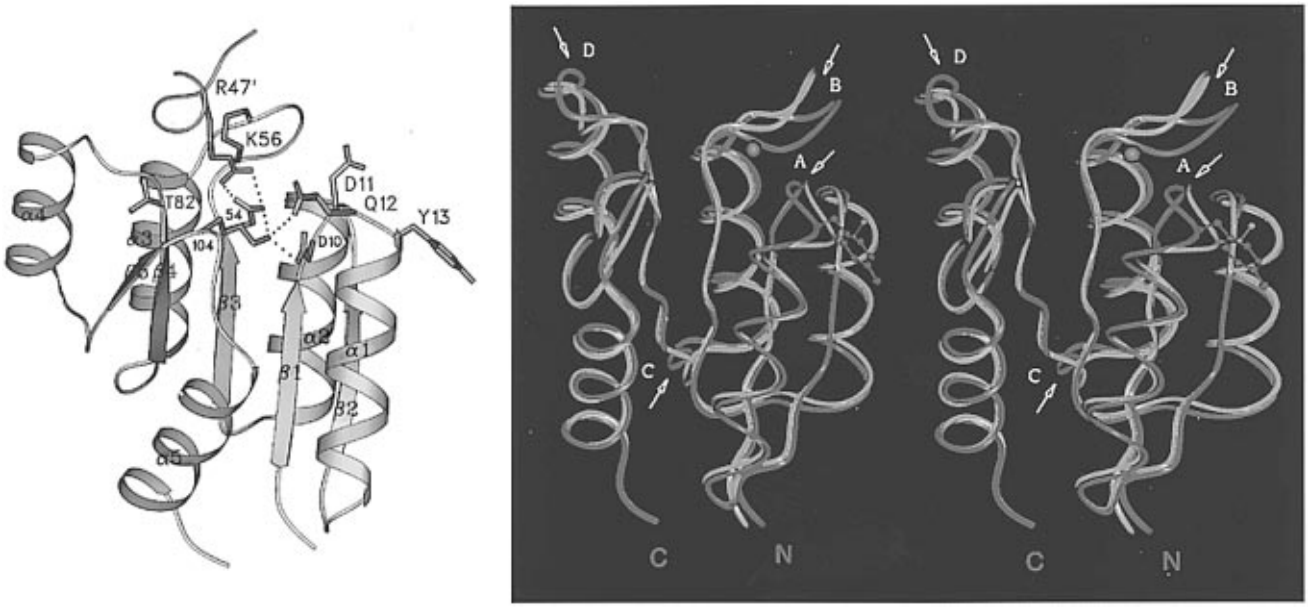

FIGURE 1: Overall structure of metal-free Spo0F and a comparison with the metal-bound form. (A, left) Ribbon diagram of the apo wild-type Spo0F molecule. Side chains of active site residues are shown along with Tyr13 and Arg47′ from the neighboring molecule. Hydrogen bonds between the side chains of the active site as well as intermolecular hydrogen bonds involving the guanidinium group of Arg47′ are depicted as broken lines. This figure was generated with SETOR (Evans, 1993). (B, right) Ribbon representation of the superposition of the apo wild-type (green) and Ca^{2+}-bound Spo0F Y13S (red) structures. The four regions where the two structures differ significantly, in the vicinity of the $\beta1-\alpha1$ loop, the $\beta3-\alpha3$ loop, the $\beta3-\alpha4$ loop, and the $\beta4-\alpha4$ loop, are designated as A−D, respectively. The calcium ion is shown in magenta. Tyr13 of the wild type and Ser13 of the mutant are also shown.

and the carbonyl oxygen of Lys56 (Figure 2A). Despite a general structural similarity, response regulators exhibit a wide range of biochemical properties, a fact which may reflect the diverse nature of functional roles played by response regulators. For example, Spo0F binds Mg^{2+} ($K_d \sim 20$ mM) 40-fold less than CheY ($K_d \sim 0.5$ mM) (Feher et al., 1995; Lukat et al., 1990). Spo0F also appears to bind Ca^{2+} ($K_d \sim 6$ mM) (unpublished results) with a 15-fold lower affinity than CheY ($K_d \sim 0.4$ mM) (Needham et al., 1993), hinting that Spo0F binds all cations more weakly than CheY. Physiological concentrations of Mg^{2+} and Ca^{2+} in bacteria are estimated to be around 1 mM and 0.1 μM, respectively (Alatossava et al., 1985; Norris et al., 1991). The concentrations of other divalent cations may also fall in this range. The high dissociation constants of Spo0F for divalent cations imply that a significant portion of the protein may not be bound to cations in the cell. We therefore think it is important to report the crystal structure of Spo0F in an uncomplexed form, possibly the predominant biological state.

EXPERIMENTAL PROCEDURES

The protein expressed in *Escherichia coli* following procedures described earlier (Zapf et al., 1996; Burbulys et al., 1991) was purified to homogeneity in high yield by a two-step purification procedure employing DEAE-trisacryl and hydroxyapatite chromatography. The crystals were grown at 4 °C by the hanging drop procedure. The drops were formed by mixing 2 μL of protein at 15 mg/mL with a 2 μL reservoir solution that contained 25% PEG 4500 and 15% ethanol in 100 mM $KNaPO_4$ buffer at pH 7.8. These conditions are different from those employed for the derivation of Y13S mutant crystals, which were obtained at pH 4.5 (Madhusudan et al., 1996a). The space group was determined using precession techniques on a multiwire area detector (Howard et al., 1985). The crystal data are as follows: space group $P4_22_12$, $a = b = 58.5$ Å, and $c = 85.4$ Å, with one molecule per asymmetric unit. The crystals diffracted to 2.45 Å resolution, and the data were measured with one crystal using a multiwire area detector system. Diffraction statistics are listed in Table 1.

The structure of the wild-type protein was solved by molecular replacement techniques using the X-PLOR suite of programs (Brunger, 1992) with the Y13S structure as a search model at 3 Å. The structure was initially refined with the program X-PLOR by rigid body refinement techniques, and it reduced the *R*-factor to 36 from 42%. Subsequently, the structure was refined by simulated annealing techniques. During refinements, omit maps were computed and several regions were rebuilt, especially near the active site. After six cycles of simulated annealing and rebuilding, the *R*-factor converged at 18.1% for 2.45 Å data. At this stage, the diffraction data were corrected for anisotropic temperature factors using the program package X-PLOR and subsequent *B*-factor refinements reduced the *R*-factor to 17.6%. The rms deviations in bond lengths and angles are 0.017 Å and 1.8°, respectively. Two residues in the N-terminal and three residues in the C-terminal of the polypeptide chain were missing in the electron density map. A typical portion of the electron density map is shown in Figure 2B. The refinement statistics are presented in Table 1. The analysis of the structure using the program PROCHECK (Laskowski et al., 1993) revealed that all the residues are in the allowed regions of a Ramachandran plot, with 90.9% residues in the most favored regions and the remaining 9.1% in additionally allowed regions. We should mention that we could not solve the present structure using the CheY structure (Volz & Matsumura, 1991) as a search model, even though the folding of the two structures is similar, as there are significant differences in the three-dimensional structures of the two molecules, especially the disposition of helixes α4 and α5 (Madhusudan, 1996b). The rms deviation between the

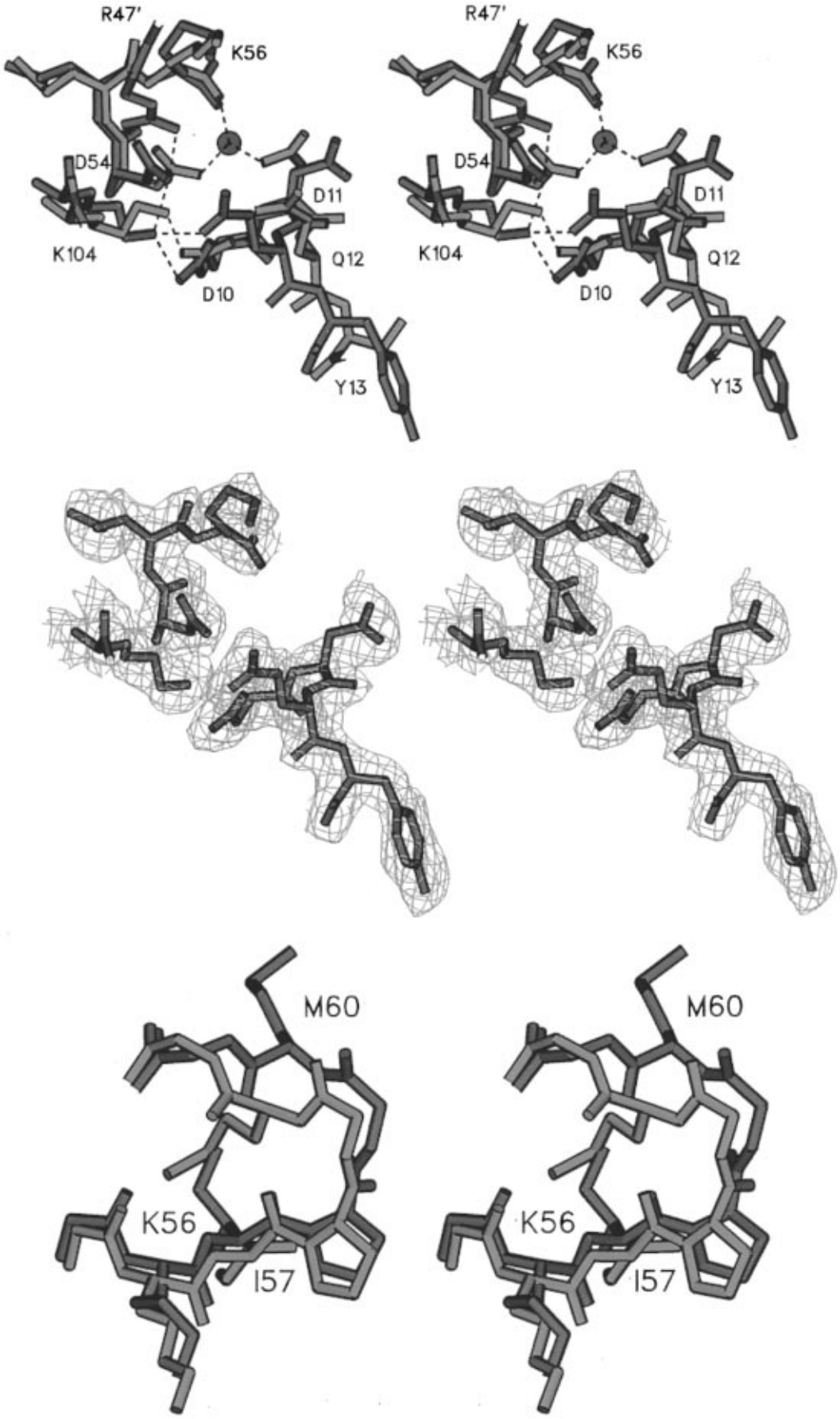

FIGURE 2: Active site and the $\beta3-\alpha3$ loop of metal-free and metal-bound forms. The figure was generated using SETOR (Evans, 1993). (A, top) Stereoview of the superposition of the active site of the apo wild-type (green) and Ca^{2+}-bound (red) Spo0F Y13S structures. Ca^{2+} coordination and hydrogen bonds are depicted in broken lines. (B, middle) Stereoview of a final $2F_o - F_c$ map for the active site residues contoured at the 1σ level. (C, bottom) Stereoview of the superposition of the $\beta3-\alpha3$ loop of the apo wild-type and Ca^{2+}-bound mutant Spo0F structures. The side chains of residues Lys56, Ile57, Pro58, and Met60 are shown.

Table 1: Data Collection and Refinement Statistics

data collection	
space group	$P4_22_12$
maximum resolution	2.45 Å
number of measured reflections	24 763
number of unique reflections	5449
R_{sym}[a]	5.7%
redundancy	4.5
$I/\sigma(I)$ at the highest shell (2.67−2.45 Å)	4.2
refinement	
resolution range	8.0−2.45 Å
number of reflections used in refinement $[F > 2\sigma(F)]$	4935
number of protein atoms	944
number of water molecules	20
crystallographic *R*-factor	17.6%
rmsd from ideal bond lengths	0.017 Å
rmsd from ideal bond angles	1.8°
average temperature factor for protein atoms	23.8 Å^2

[a] R_{sym} is a measure of the agreement among multiple observations and is calculated as $\sum(I_{ave} - I)/\sum I_{ave}$ for all reflections with multiple observations.

present structure and CheY (Volz & Matsumura, 1991) is 2.8 Å.

To perform fluorescence quenching studies to discern ligand binding, we constructed a Y13W mutant of Spo0F by the Kunkel method of site-directed mutagenesis (Kunkel et al., 1987) using the Muta-Gene Kit (BioRad) and a mutagenic primer (5′-CGTTGATGATCAATGGGGCAT-TCGTATTTTGC-3′). Quenching experiments were performed with Spo0F Y13W protein in 50 mM HEPES (pH 7.0) and 250 mM KCl (fluorescence buffer) by the addition of 0.5 M $MgCl_2$ or arginine as the ligand. Alternatively, Spo0F Y13W in the same buffer plus saturating amounts of $MgCl_2$ was titrated by the addition of 0.5 M arginine and 0.1 M $MgCl_2$ as the ligand. All ligand solutions were at pH 7.0 in fluorescence buffer and were filtered to remove particulates. The samples were excited at 295 nm (band width of 5 nm), and the emission maximum at 353 nm (band width of 10 nm) did not shift during the titration. Identical titrations of ligand versus glycyltryptophan were used to correct titration data for inner-filter effects (Ward, 1985). Nonlinear least-squares analysis was used to determine apparent ligand dissociation constants from the fluorescence quenching data (Needham et al., 1993; Ward, 1985) by employing the following relationship:

$$F_0/F = 1 + M[\mathrm{L}]/([\mathrm{L}] + K_d) + N[\mathrm{L}] \qquad (1)$$

where F and F_0 are the fluorescence intensities in the presence and absence of ligand, respectively, [L] is the free ligand concentration, M is the inverse of the fraction of total fluorescence quenched F_0/F at saturating ligand concentrations, and N is a nonspecific term that was included to account for possible dynamic or collisional quenching. All measurements were made at 20 °C using a Perkin-Elmer 650-40 spectrofluorometer.

RESULTS AND DISCUSSION

Comparison with the Ca^{2+}-Bound Mutant Spo0F Structure. Spo0F takes up a parallel (α/β) fold with an acid pocket formed by Asp10, Asp11, and Asp54 in the cavity at the carboxyl end of the β-sheet. The global fold and definition of the secondary structural elements of this molecule (Figure 1A) are identical with the structure of Ca^{2+}-bound Spo0F (Madhusudan et al., 1996b). The rms deviation between α-carbons in these two structures is only 0.94 Å. These results indicate that the scaffold of Spo0F is unaltered by Ca^{2+} binding or the Tyr13 to Ser mutation. Despite this similarity, the two Spo0F structures show rms deviations of greater than 1.0 Å in four discrete regions of the polypeptide backbone (Figure 1B). Three of these regions are localized near the active site in or adjacent to loops connecting β-strands to α-helixes, and the remaining region, the α3−β4 loop defined by residues 73−76, is located on the side of the molecule opposite from the active site. The three regions near the active site are (i) the N terminus of α1 (residues 12−15), (ii) the loop connecting β3 to α3 (residues 57−61), and (iii) the loop connecting β4 to α4 (residues 83−85). The primary causes for differences in residues 12−15 and 57−61 appear to be the point mutation Y13S and metal coordination in the mutant structure, while the differences in residues 73−76 and 83−85 appear to be caused by crystal packing. These differences with respect to the previously reported mutant structure as well as other prominent features of the wild-type structure are highlighted below.

A mutation of Tyr13 to Ser makes Spo0F resistant to the action of RapA phosphatase (Perego et al., 1994; Perego & Hoch, 1996). As the side chain of Tyr points externally away from the active site (Figure 1A), we believe its role is in interacting and positioning the RapA phosphatase, which dephosphorylates Spo0F-P. The Tyr13 to Ser mutation seems to have structural effects that extend to adjacent residues. In the present structure, the side chain of Tyr13 projects away from the active site with a χ_1 angle of −174° and packs against helix α1, whereas in the Ca^{2+}-bound Spo0F Y13S structure, the hydroxyl group of Ser13 points toward its own main chain amide nitrogen with a χ_1 angle of −26° (Figure 2A). Because of the hydrophobic nature of the tyrosine side chain, full extension of it into the solvent is not favorable, and hence, it adheres to the outer surface of α1. Furthermore, the β1−α1 loop preceding Tyr13 is shifted toward the active site in the apo structure relative to its position in the Ca^{2+}-bound structure (Figure 1B). This shifted position of the loop is stabilized by a hydrogen bond between the carboxyamide of Gln12 and Nζ of Lys104 which extends toward this loop (Figure 2A).

A comparison of the coordination site of the Y13S mutant with the corresponding region in the present wild-type apo form is shown in Figure 2A. All three coordinating atoms from the protein have moved away from the site of coordination in the apo structure. The most significant change is in the orientation of the Asp11 side chain, which points away from the site of coordination in the apo structure with a χ_1 side chain torsion angle of −167° compared to −69° in the calcium-bound structure. The other two coordinating atoms, the carbonyl of Lys56 and the carboxylate of Asp54, move away by 0.80 and 1.76 Å, respectively.

The displacement of the Lys56 carbonyl by 0.8 Å, accompanied by the changes in the main chain torsion angles, is perhaps responsible for the larger displacement (1.8−3.1 Å for α-carbons) of the subsequent residues (57−61) in the β3−α3 loop (Figure 1B). There are no crystal contacts in this region that could account for this movement, and the NMR results with Spo0F also suggest the divalent cation induces changes in this loop since the chemical shifts of

residues in this region are altered by the addition of Mg^{2+} (Feher et al., 1995). The loss of the coordinating interaction between the metal and Lys56 allows this residue to move to a new position in the metal-free structure. As a consequence of the movement in the $\beta3-\alpha3$ loop, the side chain of Ile57 rotates into the position occupied by the side chain of Met60 in the Ca^{2+}-bound Spo0F structure (Figure 2C). Thus, the side chain of Met60 is squeezed out from a buried to a solvent-exposed position, resulting in a displacement of over 9.0 Å for the Cϵ atom. The Met side chain has a high-temperature factor of 45 Å^2, but it is well-defined in the electron density map. The functional significance of this side chain switching, if any, is not known.

In the present apo Spo0F structure, the disposition of the side chain of Lys104 is a prominent feature of the active site, being in a fully extended conformation and forming hydrogen bond contacts with Asp10, Asp54, and Gln12. The staggered orientation of hydrogen bond acceptors creates a favorable environment for strong interactions between the Nζ of Lys104 and the carboxylates of Asp10, Asp54, and the carboxyamide of Gln12, which have N$\cdots$O distances of 2.83, 2.65, and 3.19 Å, respectively. The excellent hydrogen bonding interactions of the Nζ of Lys104 gives rigidity to the Lys104 side chain with a low-temperature factor of 4 Å^2. Two of these contacts are disrupted by divalent cation binding, while only the contact between Lys104 and Asp10 is preserved in the Ca^{2+}-bound structure. Consistent with an active site location, Lys104 is absolutely conserved among response regulators, but its function has yet to be fully defined (Volz, 1993; Drake et al., 1993). Mutation of the equivalent residue in CheY, Lys109 to Arg or Gln, results in mutant proteins that can be phosphorylated in a manner similar to that of the wild-type protein but are unable to generate the proper flagellar motor response (Lukat et al., 1991; Welch et al., 1994). The conformation of the side chain of this invariant Lys appears to be sensitive to its environment as the introduction of a divalent cation or mutations at the active site (Bellsolell et al., 1994) alter the conformation. An adaptable side chain conformation may be essential for this residue to form critical interactions in the phosphorylated protein. The nature of these contacts cannot be predicted from the unphosphorylated structure, but they appear to be important for generating an active conformation after phosphorylation (Lukat et al., 1991).

Another significant change in the active site is the fact that the side chain of Thr82 takes up a rotamer state with a χ_1 of 175° (for the hydroxyl) compared to 73° in the metal-bound structure. Similar differences are observed in the metal-free and metal-bound structures of *E. coli* CheY (Volz, 1995), despite the residue being distal from the coordination site. This is especially noteworthy because this residue has been shown to be essential for generating an active form of response regulators after phosphorylation (Ganguli et al., 1995).

Comparison with CheY Structures. Spo0F binds Mg^{2+} and Ca^{2+} with K_d values of 23 and 6 mM, respectively, whereas CheY binds Mg^{2+} and Ca^{2+} with K_d values of 0.5 and 0.4 mM, respectively (Feher et al., 1995; Lukat et al., 1990; Needham et al., 1993). In the CheY$-Mg^{2+}$ complex (Stock et al., 1993), the magnesium ion is octahedrally coordinated to six oxygen atoms with an average $Mg^{2+}\cdots$O distance of 2.15 Å. In the Spo0F Y13S$-Ca^{2+}$ complex, the geometry of coordination is less favorable, with only five oxygens coordinating to calcium, giving a distorted octahedral geometry and an average $Ca^{2+}\cdots$O distance of 2.23 Å. Thus, the weaker affinity of Spo0F for divalent cations may be linked to the observed nonideal geometry of coordination. In CheY, the Mg^{2+} is coordinated to three protein oxygens, the side chain carboxyl oxygens of Asp13, Asp57, the carbonyl of Asn59, and three water molecules. A comparison of the apo structure of CheY with the two Mg^{2+}-bound structures of CheY shows that the carbonyl of Asn59 (the equivalent position in Spo0F is 56) has the same orientation in all three structures. The dispositions of the Asp13 and Asp57 side chains in the two Mg^{2+}-bound structures are nearly the same, while they are oriented slightly differently in the apo structure (Volz, 1995). The rearrangement of the side chains can take place with very little energy cost. Therefore, in CheY, the ion binding cavity can be readily formed with excellent coordinating geometry. In contrast, the carbonyl oxygen of Lys56 in the metal-bound form of Spo0F is displaced by 0.8 Å (Figure 2A) with respect to the metal-free form. Therefore, the coordination necessitates a change in the polypeptide backbone conformation. Hence, the formation of the coordination cavity is more complex in Spo0F and less favorable due to nonideal coordination geometry. Thus, it appears that the Spo0F active site is designed to bind divalent cations with weak affinity. The functional role of this physical property, if any, in the signaling process controlling sporulation remains speculative. In Ca^{2+}-activated signaling mechanisms (Clapham, 1995), transient increases in the Ca^{2+} concentration trigger signaling cascades. One mechanism by which these signaling cascades are initiated is by Ca^{2+} binding to effector proteins and inducing a conformational change in the effector molecule (Clapham, 1995). A signaling role for Ca^{2+} in the chemotaxis system (Tisa & Adler, 1992, 1995) also has been reported. Both chemotaxis in *E. coli* (Tisa & Adler, 1995) and sporulation in *B. subtilis* (Norris et al., 1991) are Ca^{2+}-dependent processes. A calmodulin-like activity is involved in the sporulation of *Bacillus cereus* (Norris et al., 1991), implying that calcium concentrations are regulated during the sporulation process. According to the Ca^{2+} signaling paradigm, the low divalent cation binding affinity of Spo0F would ensure that the response regulator remains in the inactive "off state" until rising concentrations of the appropriate divalent cation force binding at the Spo0F active site and thus allow signaling by inducing the "on state" of the response regulator. Such a regulatory mechanism could afford another level of control over the sporulation phosphorelay.

Arginine Interaction at the Active Site. One of the most intriguing aspects of the wild-type structure is the protrusion of the Arg47′ side chain from a symmetry-related molecule ($-x+{}^1/_2, y+{}^1/_2, -z+{}^1/_2$) of Spo0F into the active site where it forms a pair of salt bridge interactions with the carboxylate of Asp54 (with N$\cdots$O distances of 2.85 and 3.14 Å), an invariant residue among response regulators that is the site of phosphorylation (Figures 1A and 2A). Figure 3 depicts a charge surface representation of Spo0F, and it shows how the positively charged arginine enters and fits the active site. Quenching of Spo0F Y13W fluorescence by free arginine suggests that this interaction occurs in solution also (Figure 4). Since wild-type Spo0F does not contain any tryptophan, Tyr13 was changed to Trp by site-directed mutagenesis in order to incorporate a fluorescence probe near the protein

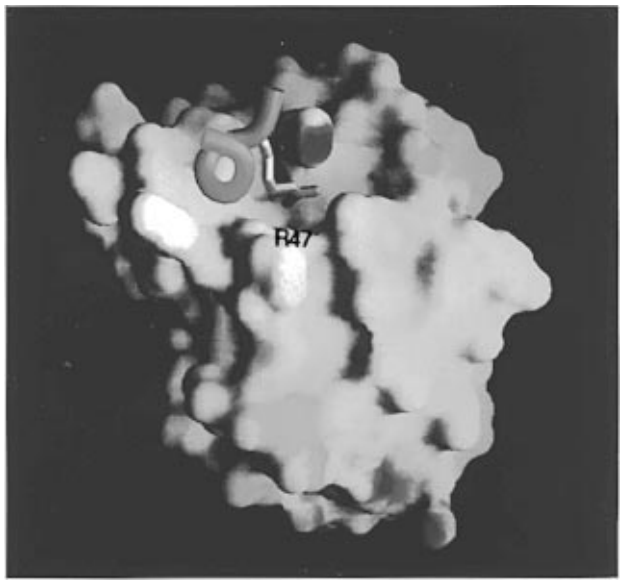

FIGURE 3: Electrostatic surface diagram of Spo0F generated by the program GRASP (Nicholls et al., 1991). Negative charges are shown in red and positive charges in blue. The entry of Arg47′ from the neighboring molecule into the active site is shown in a stick representation. It sits on top of Asp54, shown as a red patch at the bottom of the pocket. The fragment (42−48) of the neighboring molecule is shown in a worm representation in green.

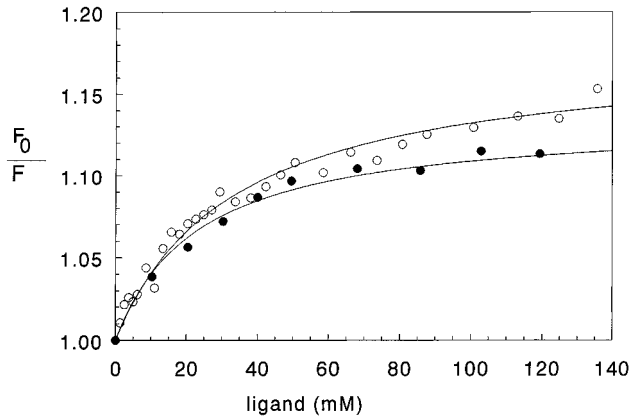

FIGURE 4: Quenching of Spo0F Y13W fluorescence by added Mg^{2+} (○) and arginine (●). Quenching experiments were performed as described in Experimental Procedures. F_0 and F correspond to the fluorescence in the absence and presence of ligand, respectively. The lines represent nonlinear least-squares fits to eq 1 yielding the following constants: Mg^{2+} as the ligand, $K_d = 23$ mM, $M = 0.13$, $N \sim$ zero; arginine, $K_d = 15$ mM, $M = 0.11$, $N = 0.000\ 42$ mM^{-1}. Since the dissociation constants are more than 1000-fold higher than the protein concentration, the ligand stoichiometry cannot be obtained (Ward, 1985).

active site. The surface location of this residue in the protein structure obviates any steric problems caused by the bulky tryptophan side chain. The mutant Spo0F Y13W was phosphorylated by the sporulation histidine kinase, KinA, and upon phosphorylation, it transferred phosphate to the downstream target protein, Spo0B, in a manner indistinguishable from that of the wild-type protein. A further indication that this mutation did not disrupt the protein structure is the fact that the dissociation constant for Mg^{2+} binding to Spo0F Y13W (23 mM) as determined by fluorescence quenching is nearly identical with the value (20 mM) determined for Mg^{2+} binding to the wild-type protein by NMR (Feher et al., 1995). The fluorescence quenching experiments (Figure 4) suggest that structural features of the arginine side chain are responsible for the specificity of this interaction as only arginine appears to bind to Spo0F in a saturable manner ($K_d = 15$ mM), whereas other amino acids (Gln, Met, Lys, and His) do not. Furthermore, the quenching of Spo0F Y13W fluorescence by free arginine can be blocked by saturating amounts (100 mM) of Mg^{2+}, implying that arginine and Mg^{2+} compete for the same binding site (data not shown). The insertion of Arg47′ appears to cause the displacement of the loop connecting β4 and α4 (residues 83−85) by up to 4.6 Å. We do not see any direct influence of metal binding on the displacement of the loop, as there are no contacts between the cation and this loop. However, NMR studies on CheY (Moy et al., 1994) show that there are conformational differences in this loop region between metal-bound and metal-free structures. NMR studies on Spo0F (Feher et al., 1995) are also indicative of conformation flexibility at this region.

Conclusions. Baikalov et al. (1996) have recently solved the crystal structure of the response regulator NarL, which consists of both the receiver domain and the output domain. The overall structure of the receiver domain of NarL is similar to two other response regulatory proteins Spo0F and CheY. It has been reported that NarL and CheY differ significantly in their orientation of helix α5. In NarL, helix α5 is oriented away from helix α4 by 21° compared to that in the CheY structure. The dispositions of helixes α4 and α5 are remarkably similar in Spo0F and NarL. This similarity is also reflected in a lower rms deviation of 1.8 Å for their equivalent α-carbon positions compared to a larger rms deviation of 2.8 Å between Spo0F and CheY. Furthermore, the disposition of Asp11 in the metal-free structure of Spo0F is similar to that of the equivalent residue, Asp14, in the metal-free structure of NarL. In both structures, their carboxylates point away from the active site. It appears that for Spo0F and NarL the metal binding site is not preformed but it is induced upon metal binding. This might be the general feature of response regulatory proteins.

As the incidence of bacterial drug resistance is on the rise (Service, 1995), there is a renewed interest in the development of antimicrobial agents. Since two-component systems are vital to the survival of bacteria and lower eukaryotes, members of these signaling pathways are potential drug targets (Roychoudhury et al., 1993). Significantly, binding of Arg47′ at the Spo0F active site provides insight into the type of interactions that can be exploited in the design of inhibitors of response regulators. Our observation suggests that peptidomimetics with guanidinium moieties may function to block two-component systems. The difference between this and the previously reported structure of Ca^{2+}-bound Spo0F Y13S establishes the fact that significant structural changes take place on metal binding. The movements generating this conversion appear to be localized to amino acid side chains and loops near the divalent cation binding active site. These conformational changes are a prerequisite for the phosphosignaling reactions catalyzed by response regulators.

ACKNOWLEDGMENT

We thank Alan Kinkaid and Edwina Kentabe for technical assistance.

REFERENCES

Alatossava, T., Jutte, H., Kuhn, A., & Kellenberger, E. (1985) *J. Bacteriol. 162*, 413−419.

Alex, L. A., Borkovich, K. A., & Simon, M. I. (1996) *Proc. Natl. Acad. Sci. U.S.A. 93*, 3416−3421.

Baikalov, I., Schroder, I., Kaczor-Grzeskowiak, M., Greskowiak, K., Gunsalus, R. P., & Dickerson, R. E. (1996) *Biochemistry 35*, 11053−11061.

Bellsolell, L., Prieto, J., Serrano, L., & Coll, M. (1994) *J. Mol. Biol. 238*, 489−495.

Bellsolell, L., Cronet, P., Majolero, M., Serrano, L., & Coll, M. (1996) *J. Mol. Biol. 257*, 116−128.

Brünger, A. T. (1992) *X-PLOR Version 3.1*, Yale University, New Haven, CT.

Burbulys, D., Trach, K. A., & Hoch, J. A. (1991) *Cell 64*, 545−552.

Clapham, D. E. (1995) *Cell 80*, 259−268.

Drake, S. K., Bourret, R. B., Luck, L. A., Simon, M. I., & Falke, J. J. (1993) *J. Biol. Chem. 268*, 13081−13088.

Evans, S. V. (1993) *J. Mol. Graphics 11*, 134−138.

Feher, V. A., Zapf, J. W., Hoch, J. A., Dahlquist, F. W., Whiteley, J. M., & Cavanagh, J. (1995) *Protein Sci. 4*, 1801−1814.

Ganguli, S., Wang, H., Matsumura, P., & Volz, K. (1995) *J. Biol. Chem. 270*, 17386−17393.

Grimsley, J. K., Tjalkens, R. B., Strauch, M. A., Bird, T. H., Spiegelman, G. B., Hostomsky, Z., Whiteley, J. M., & Hoch, J. A. (1994) *J. Biol. Chem. 269*, 16977−16982.

Hoch, J. A. (1993) *Annu. Rev. Microbiol. 47*, 441−465.

Howard, A. J., Nielsen, C., & Xuong, N. H. (1985) *Methods Enzymol. 114*, 452−472.

Kunkel, T. A., Roberts, J. D., & Zakour, R. A. (1987) *Methods Enzymol. 154*, 367−382.

Laskowski, R. A., MacArthur, M. W., Moss, D. S., & Thornton, J. M. (1993) *J. Appl. Crystallogr. 26*, 283−291.

Lukat, G. S., Stock, A. M., & Stock, J. B. (1990) *Biochemistry 29*, 5436−5442.

Lukat, G. S., Lee, B. H., Mottonen, J. M., Stock, A. M., & Stock, J. B. (1991) *J. Biol. Chem. 266*, 8348−8354.

Madhusudan, Zapf, J., Whiteley, J. M., Hoch, J. A., Xuong, N. H., & Varughese, K. I. (1996a) *Acta Crystallogr. D 52*, 589−590.

Madhusudan, Zapf, J., Whiteley, J. M., Hoch, J. A., Xuong, N. H., & Varughese, K. I. (1996b) *Structure 4*, 679−690.

Moy, F. J., Lowry, D. F., Matsumura, P., Dahlquist, F. W., Krywko, J. E., & Domaille, P. J. (1994) *Biochemistry 33*, 10731−10742.

Needham, J. V., Chen, T. Y., & Falke, J. J. (1993) *Biochemistry 32*, 3363−3367.

Nicholls, A., Sharp, K. A., & Honig, B. (1991) *Proteins 11*, 281−296.

Norris, V., Chen, M., Goldberg, M., Voskuil, J., McGurk, G., & Holland, I. B. (1991) *Mol. Microbiol. 5*, 775−778.

Parkinson, J. S., & Kofoid, E. C. (1992) *Annu. Rev. Genet. 26*, 71−112.

Perego, M., & Hoch, J. A. (1996) *Trends Genet. 12*, 97−101.

Perego, M., Hanstein, C., Welsh, K. M., Djavakhishvili, T., Glaser, P., & Hoch, J. A. (1994) *Cell 79*, 1047−1055.

Roychoudhury, S., Zeilinski, N. A., Ninfa, A. J., Allen, N. E., Jungheim, L. N., Nicas, T. I., & Chakrabarty, A. M. (1993) *Proc. Natl. Acad. Sci. U.S.A. 90*, 965−969.

Santoro, J., Bruix, M., Pascual, J., Lopez, E., Serrano, L., & Rico, M. (1995) *J. Mol. Biol. 247*, 717−725.

Service, R. F. (1995) *Science 270*, 724−727.

Stock, A. M., Mottonen, J. M., Stock, J. B., & Schutt, C. E. (1989) *Nature 337*, 745−749.

Stock, A. M., Martinez-Hackert, E., Rasmussen, B. F., West, A. H., Stock, J. B., Ringe, D., & Petsko, G. A. (1993) *Biochemistry 32*, 13375−13380.

Stock, J. B., Stock, A. M., & Mottonen, J. M. (1990) *Nature 344*, 395−400.

Swanson, R. V., Alex, L. A., & Simon, M. I. (1994) *Trends Biochem. Sci. 19*, 485−490.

Tisa, L. S., & Adler, J. (1992) *Proc. Natl. Acad. Sci. U.S.A. 89*, 11804−11808.

Tisa, L. S., & Adler, J. (1995) *Proc. Natl. Acad. Sci. U.S.A. 92*, 10777−10781.

Volkman, B. F., Nohaile, M. J., Amy, N. K., Kustu, S., & Wemmer, D. E. (1995) *Biochemistry 34*, 1413−1424.

Volz, K. (1993) *Biochemistry 32*, 11741−11753.

Volz, K. (1995) in *Two-Component Signal Transduction* (Hoch, J. A., & Silhavy, T. J., Eds.) pp 53−64, ASM Press, Washington, DC.

Volz, K., & Matsumura, P. (1991) *J. Biol. Chem. 266*, 15511−15519.

Ward, L. D. (1985) *Methods Enzymol. 117*, 400.

Welch, M., Oosawa, K., Aizawa, S. I., & Eisenbach, M. (1994) *Biochemistry 33*, 10470−10476.

Zapf, J. W., Hoch, J. A., & Whiteley, J. M. (1996) *Biochemistry 35*, 2926−2933.

BI971276V